Polymer Degradation and Stability 216 (2023) 110485

Contents lists available at ScienceDirect

Polymer Degradation and Stability

journal homepage: www.journals.elsevier.com/polymer-degradation-and-stability

Early stages of X-ray induced molecular unit modifications in poly (lactic acid)

Giulia Tamburini [a], Stefano Bertagnoli [b], Giulia Tarricone [a], Sergio Piva [a], Adele Sassella [a], Roberto Lorenzi [a,*], Alberto Paleari [a]

[a] Department of Materials Science, University of Milano-Bicocca, Via Cozzi 55, Milano 20125, Italy
[b] Galatea Bio Tech Srl, Piazza della Scienza 2, U4, Milano 20126, Italy

ARTICLE INFO

Keywords:
Poly(lactic acid)
Radiation damage
FTIR spectroscopy
X-ray irradiation

ABSTRACT

Exposure of polymers to ionizing radiation and high-energy particle beams is involved in many processes – from food sterilization to radiotherapy protocols. The resulting effects, at the final stages, determine the functional, structural, and morphological alteration of the material. However, the processes responsible for cumulative chain scission, crosslinking, and reactions with the environment are often difficult to disentangle as a sequence of elementary events. Here we report a spectroscopic study – by attenuated-total reflection Fourier transform infrared spectroscopy and powder x-ray diffraction measurements, together with differential scanning calorimetry and thermogravimetric analyses – that sheds light on the very initial stages of the mechanisms involved in radiation-induced modifications of poly(lactic acid) (PLA). The results, collected on samples from biobased processes and exposed to low x-ray doses in the range of 10^0–10^3Gy after different thermal treatments, show spectroscopic evidence of the emergence of molecular unit perturbations – mainly related to methyl and carbonyl groups with the formation of C=C double bonds – with a clear-cut dependence on the polymer conformation. Understanding the mechanisms involved and the role of crystallinity provides information potentially useful for the development of PLA with a suitable radiation hardness for applications in radiotherapy.

1. Introduction

Ionizing radiation is involved in plenty of applications of polymeric materials, and in the last decades several works have been devoted to the analysis of radiation-induced effects on the mechanical and functional properties of polymers, including hardness and plasticity, dielectric response, color, and micromorphology [1]. The understanding of the underlying mechanisms – including the role of the crystalline or amorphous state as a promoting or inhibiting factor of modification – is important to optimize materials and processes in view of specific applications. This aspect is particularly relevant for those polymers which are potentially interesting as biodegradable carriers of radioisotopes for internal radiotherapy.

In this field, inorganic glass microspheres have been clinically employed up to now – despite some disadvantages related to the relatively high density of glass compared to blood plasma – thanks to their biocompatibility, good chemical stability, and radiation hardness which ensures negligible leaching of incorporated radioisotopes [2–5]. However, the very slow biodegradation of glass-based systems results in a relatively long residence time in the organism, which limits the prescription of treatment cycles, as well as any kind of efficient treatment optimization through preliminary diagnostic phases, with low-dose pilot microspheres. To overcome these limitations, the use of biodegradable polymeric microspheres in internal radiotherapy could represent an important complementary tool enabling pre-therapeutic phases which constitute the essential step to achieve sustainable personalized oncological therapies.

However, even though many studies have been carried out in the last years on important medical applications of polymers – mainly as carriers for drug delivery [6–8], nanoparticles for theragnostic imaging [9], and in the production of medical devices [10] – relevant questions need to be addressed before they can be used as radioisotope microcarriers. The most important issue concerns achieving a delicate balance between biodegradability and radiation hardness – the former enabling fast removal of the microspheres from the organism, the latter preventing possible leaching of the radioisotope before its radioactivity decay. The

* Corresponding author.
E-mail address: roberto.lorenzi@unimib.it (R. Lorenzi).

https://doi.org/10.1016/j.polymdegradstab.2023.110485
Received 24 April 2023; Received in revised form 30 June 2023; Accepted 20 July 2023
Available online 22 July 2023

control of these features requires a deep understanding of the mechanisms of radiation damage as a function of the initial structure which, at the same time, plays a role in the biodegradability of the polymer.

In this regard, poly(lactic acid) (PLA) has the potential to be a promising candidate for these applications thanks to its biocompatibility and high biodegradability in the human organism. Some data concerning PLA as a radionuclide microcarrier can already be found in the early investigations on microspheres for internal radiotherapy [11–14], which were then further analyzed in a few more recent works [15,16]. The available data concern a preliminary evaluation of radioisotope leaching by *in vitro* and *in vivo* experiments, and some clinical studies for the treatment of hepatic tumors. Information on the effects of radiation on PLA mainly comes from studies on PLA for different uses, which require PLA tools and films to undergo sterilization processes or functionalization treatments employing UV light, corona processes, x-ray, β, or γ beams [17–19].

Studies on the radiation effects on the structure and morphology of PLA systems mainly report changes in the molecular weight, which in turn directly point to important information on the occurrence of crosslinking and chain scission processes as final results of irradiation [20–23]. Spectroscopic results, from Fourier-transform infrared (FTIR) absorption – or attenuated total reflection (ATR) FTIR – and Raman scattering, show that crosslinking and chain scission are accompanied by spectral changes that appear as shape changes in the FTIR and/or Raman bands of the C=O and CH_3 vibrational modes [24,25]. The observed spectral changes, resulting from γ and β irradiation [26–32], underline the occurrence of perturbations in the environment of carbonyl and methyl groups resulting from radiation-induced conformational changes, leading to the degradation of the polymeric system.

The mechanisms responsible for the evidenced chain crosslinking and chain scission are related to bond breaking and the subsequent reaction between terminal groups. Norrish I and/or Norrish II processes have often been proposed as possible mechanisms [33,34], sometimes with the formation of radicals as suggested by electron paramagnetic resonance studies [29,31,32]. However, the very initial stages of the radiation-induced perturbation within the molecular unit of the polymer is still undefined. As a matter of fact, clear evidence of the nature of the initial modification occurring within the molecular unit is still lacking, since the range of low irradiation doses is largely unexplored, as is the role of the crystalline or amorphous state in these initial stages.

The aim of the present work is to shed light on the mechanisms taking place in the first steps of the molecular perturbation in irradiated PLA, especially looking at the role of polymer conformation in triggering or inhibiting the modification events, so as to find the best practices to produce PLA with suitable radiation hardness for radiotherapy applications.

2. Materials and methods

The present investigation is based on a matrix of unirradiated and irradiated PLA samples ($M_w \sim 60$ kDa) with different starting conformational features obtained by thermal treatments of a batch of semi-crystalline PLA pellets, each with a mass of 15–20 mg, fabricated by hot extrusion (180 °C) of bio-produced L-isomer. Thermogravimetric analysis (Fig. S1), using a Mettler Toledo TGA/DSC1HT STARe System, and combustion-based organic elemental analysis, by means of an Elementar VarioMicro-Cube analyzer, give evidence that the final material results to be free from bioprocess residuals, either in the form of solvents or as nitrogen- and sulfur-containing contaminants, with concentrations below the instrumental detection limit in the order of 10^2 ppm. Traces of water are present only due to the PLA hygroscopicity, as indeed revealed in a few samples by very weak broad infrared absorption in the H—O-H bending region of water molecules. Surface contamination is ruled out by comparing measurements on external and freshly cut surfaces.

Five different types of starting materials can be distinguished in the investigated sample sets – as-extruded (AE) and re-extruded (RE) PLA samples, and, starting from AE, samples heated above the melting temperature of 220 °C and then quenched at 0 °C (MQ), samples treated at 220 °C and retracted after cooling by a cold crystallization process to 150 °C (CC), and samples treated at 220 °C and remelted after cooling at 220 °C (RM). Thermal treatments of samples sealed in 40 μL aluminum pans were performed during Differential Scanning Calorimetry (DSC) measurements, using a DSC-1 system (Mettler Toledo STARe) equipped with a liquid N_2 low-temperature apparatus. Heat flow was measured during heating/cooling ramps between 0 and 220 °C at 10 °C/min under N_2 atmosphere. Indium was used as a standard for temperature and heat flow calibration. The glass transition temperature (T_g) was determined as the midpoint of the step transition in the calorimetric curve. The crystalline or amorphous state of the materials was characterized by powder x-ray diffraction (PXRD) using a Rigaku powder diffractometer equipped with a Cu-Kα source, 40 kV, and 30 mA. PXRD profiles were recorded in 2θ ranges from 5.0° – 40.0° with a step size of 0.02° and a scan speed of 2.0°min^{-1}.

Information on the PLA conformation is also provided by Raman spectroscopy using a Labram Horiba Jobin-Yvon spectrometer with a 632.8 nm HeNe laser source. The scattered light was collected with a 10x objective mounted on a microscope head (Olympus BX40) and detected by a charge coupled device (CCD-Sincerity, Jobin-Yvon) with a spectral resolution of 1 cm^{-1}.

From each set of PLA material, some of the samples have been exposed to different doses of x-ray irradiation, comprising a low dose range from 1 to 100 Gy and a higher dose range from 300 to 3000 Gy. The first x-ray dose range is completely unexplored, whereas the second one is partially overlapped to the lower limit of 1 kGy of most of previous investigated dose ranges. Lacking any information on the dose threshold for elementary events of molecular perturbation, the selected doses have tentatively been chosen with values 1×10^k Gy and 3×10^k Gy for $k = 0,1,2,3$ to sample the induced effects along a logarithmic scale of values. Irradiation have been carried out using an x-ray tube with W target, 20 kV accelerating voltage, and 20 mA current intensity. The effects of irradiation have then been analyzed by collecting attenuated total reflection Fourier-transform infrared (ATR-FTIR) spectra by means of a Thermo Fisher Nicolet iN10 infrared microscope from 675 to 4000 cm^{-1} equipped with a single crystal Ge tip. The statistical analysis of the spectral intensity is based on spectra collected at five different points on each PLA pellet, and averaged over repeated measurements on different pellets after similar treatments, for a total of more than 200 samples analyzed. In all spectra, the measured intensities are normalized with respect to the intensity of the asymmetric bending mode of CH_3 at 1450 cm^{-1}, which serves as an internal reference, since no changes in the C—H bonds of the methyl groups are expected due to the irradiation [21]. Repeated measurements have also been collected after different time periods after the irradiation, from a few minutes to several weeks, confirming the stability of the observed spectral changes at room temperature throughout the whole investigation. Further stability studies of the irradiation effects have been carried out through isochronous and isothermal annealing experiments by heating irradiated samples for 1–10 min at temperatures ranging from 50 to 80 °C.

Further information of the effect of irradiation have been collected by ^{1}H Nuclear Magnetic Resonance (NMR) and Gel Permeation Chromatography (GPC). ^{1}H NMR spectra were acquired on a Bruker Avance NEO spectrometer operating at 400.13 MHz for ^{1}H, equipped with a 5 mm broadband with fluorine probe. Deuterated chloroform, $CDCl_3$, was used as a solvent. Molecular weight distributions of PLA samples were determined by GPC using a Waters 1515 isocratic HPLC pump, with refractive index detector and four Styragel columns. A polystyrene standard (Sigma-Aldrich) was used as calibration to calculate the molecular weights.

3. Results and discussion

3.1. Initial conformation

The results of the DSC analysis provide a first overview of the thermal history and expected conformation of the investigated PLA materials before irradiation. In Fig. 1, we report representative DSC curves of the two types of starting material, namely PLA by single hot extrusion (AE sample, Fig. 1a), and PLA by double hot extrusion (RE sample, Fig. 1b). The absence of an exothermic crystallization peak during the first heating in Fig. 1a, which instead occurs in Fig. 1b at about 100 °C, reflects a predominantly crystalline state of the AE material, whereas the RE material starts from a mainly amorphous structure. Even during the cooling process to 0 °C, the AE sample does not exhibit exothermic peaks at about 105 °C, instead present in the RE sample.

Both samples show a glass transition at similar temperatures (about 64 °C) and an endothermic melting peak at 175 °C. Fig. 1a also shows how the material, starting from AE, undergoes a cold crystallization during a second heating, after melting (at 220 °C for 1 min) and cooling to 0 °C, as indicated by a broad exothermic peak at about 115 °C. This fact evidences the lowering of crystallinity after heating above the melting temperature. Interestingly, a second heating above the melting temperature during a third DSC cycle (see Fig. S2) makes the material definitely amorphous and able to give rise to an intense crystallization exo-peak similar to the peak in the first cycle of Fig. 1b. This fact suggests that the combined thermal and mechanical conditions of re-extrusion of the parent semicrystalline AE material, giving the RE sample, are assimilable to a repeated melting process with consequent amorphization of the structure. As a result of the DSC curves, AE and CC samples are expected to show crystalline features, whereas amorphous features are expected in the RE sample and in MQ and RM samples obtained from the AE sample through treatments stopped after melting. Detailed confirmation about PLA conformation within the investigated set of materials comes from powder x-ray diffraction (Fig. 2).

Comparing the PXRD patterns, well-defined peaks are detected in AE and CC samples, whereas only a broad halo is observed in samples MQ, RM, and RE. The narrow reflections at 2θ= 16° and 18° are consistent with the presence of 10_3 helices of crystalline PLA in α-form, while the broad band is typical of amorphous polymeric compounds [24,35]. Therefore, AE and CC samples are crystalline features while the other samples are amorphous, as also confirmed by Raman spectra (Fig. S3).

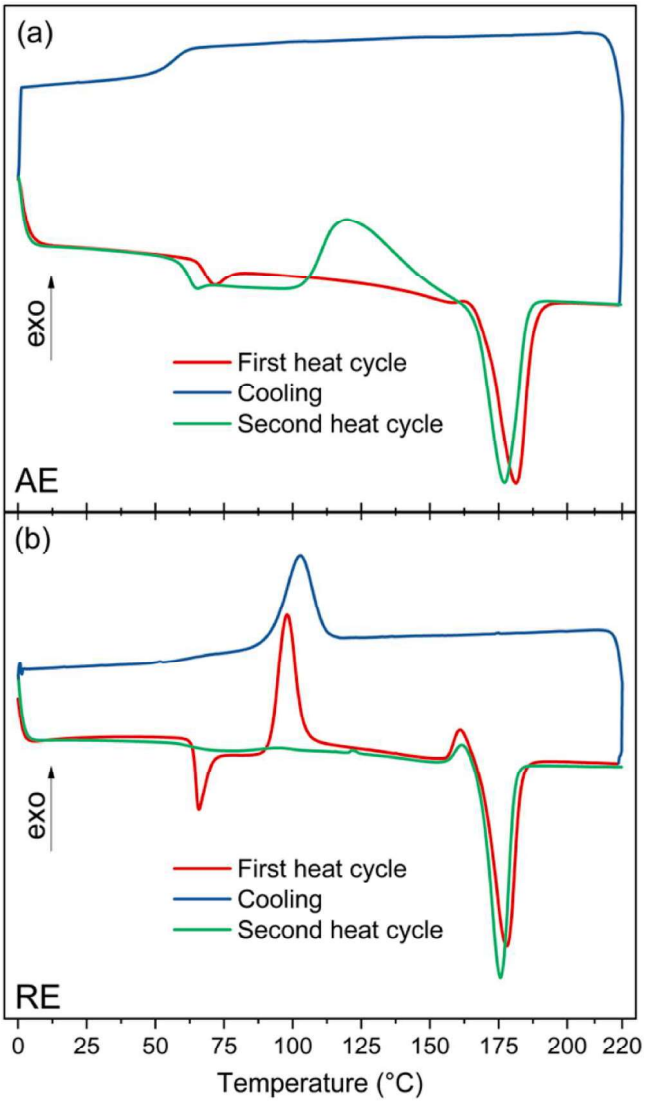

Fig. 1. DSC characterization. Cycles of differential scanning calorimetry of (a) PLA material produced by hot extrusion at 180 °C followed by slow cooling (AE sample), and (b) PLA material produced by two subsequent processes of hot extrusion at 180 °C (RE sample).

3.2. Irradiation effects

The ATR-FTIR spectra of the investigated materials register all the intrinsic spectral features of PLA (Fig. 3a). The region between 1000 and 1500 cm^{-1} is dominated by skeletal stretching modes and CH_3 rocking and bending modes, the region at around 1750 cm^{-1} shows the strong C=O stretching mode, while the expected CH_3 stretching modes are found at around 2900 cm^{-1} [24]. No relevant spectral changes are registered in these intrinsic vibrational modes after irradiation in the investigated dose range.

This outcome is also confirmed by the comparison between Raman spectra before and after irradiation (Fig. S3b). However, looking at Fig. 3b and c, weak modes are detected in irradiated material, not

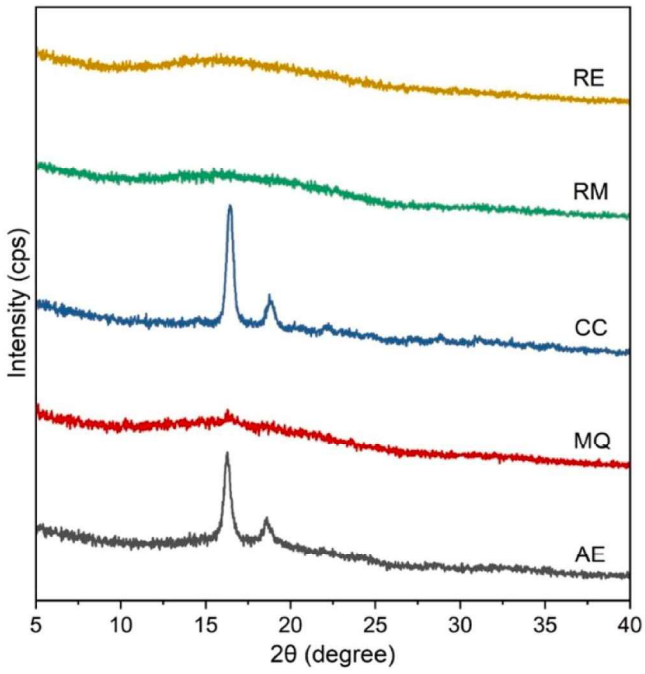

Fig. 2. PXRD. PXRD patterns in the 2θ range of 5°−40° of different types of PLA: as-extruded (AE) at 180 °C, extruded and melted at 220 °C then quenched at 0 °C (MQ), extruded and melted then cooled and subsequently cold crystallized by reheating at 150 °C (CC), extruded and melted then cooled and subsequently remelted (RM), and re-extruded (RE).

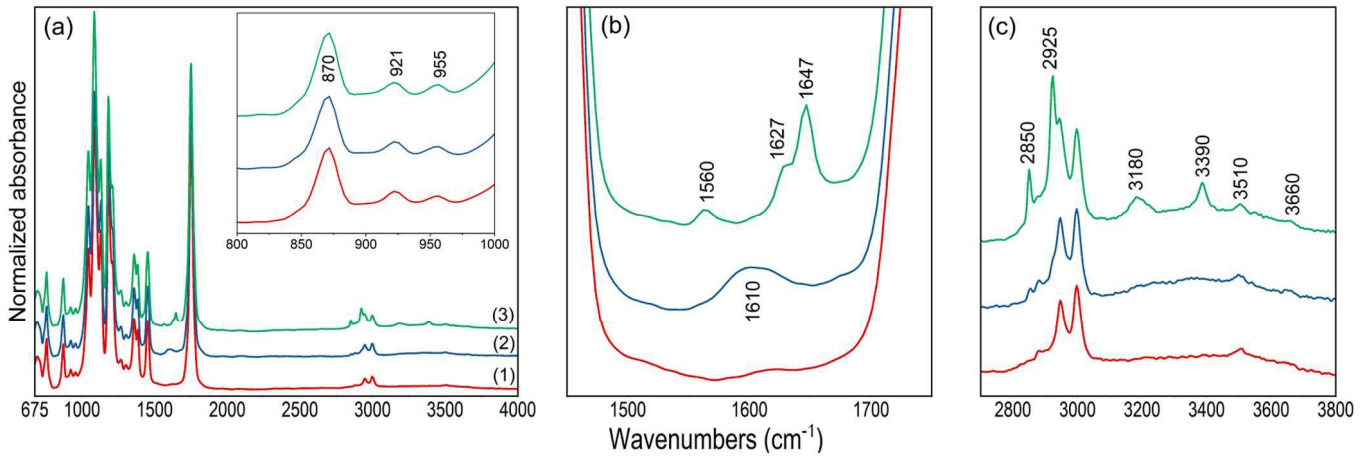

Fig. 3. Irradiation effects in infrared spectra. (a) ATR-FTIR representative spectra of (1) unirradiated PLA sample, (2) unirradiated PLA sample with native 1610 cm^{-1} band, and (3) x-ray irradiated PLA sample with additional radiation-induced peaks. Inset: magnification of the spectral region 800–1000 cm^{-1}, showing three vibrational modes associated with the CH_3 rocking mode coupled with (C—COO) stretching mode, which are highly sensitive to the chain crystallinity. All values are normalized to the intensity of the 1450 cm^{-1} peak of CH_3 bending mode. Magnifications of the regions (b) 1450–1750 cm^{-1} and (c) 2750–3800 cm^{-1}, where the positions of the relevant peaks are indicated.

belonging to the expected PLA phonon modes, at 1560 and 1610 cm^{-1}, at 1627 and 1647 cm^{-1}, at 2850 and 2925 cm^{-1}, and at 3180 and 3390 cm^{-1} (Fig. 3b and c). The detection of these peaks in the spectra of the irradiated samples is well reproducible up to a time scale of weeks.

Fig. 4 summarizes the statistics of intensity *vs.* dose experiments for all these peaks, collected in hundreds of measurements on different PLA samples of the same batch, in the range of low doses, from 0 to 100 Gy, not investigated up to now. The data show clear dependencies on the x-ray exposure, well above the uncertainty arising from the inhomogeneous and sample-dependent response of the polymeric system. Indeed, the peaks at 1560 cm^{-1}, 1627–1647 cm^{-1}, and 3180–3390 cm^{-1} result to be radiation-induced peaks, while the peak at 1610 cm^{-1} occurs randomly in unirradiated samples and, when detected before irradiation, decreases with irradiation. Instead, the peaks at 2850 and 2925 cm^{-1} are enhanced by irradiation but are also detected in some unirradiated samples. The intensity of the radiation-induced spectral features is rather high, reaching values of about 1–10% the reference intensity of the intrinsic CH_3 mode at 1450 cm^{-1}.

Further information comes from correlation plots between the intensities of the irradiation-dependent peaks, as reported in Fig. 5 for some relevant cases (further data in Figs. S4 and S5). Namely, the set of statistical data in Fig. 5 allows us to highlight the following facts. First, Fig. 5a-c point to a strict relation between three peak pairs, namely the peaks at 1627 and 1647 cm^{-1}, the peaks at 2850 and 2925 cm^{-1}, and the peaks at 3180 and 3390 cm^{-1}. These peak pairs also show a moderate correlation with each other (Fig. 5d–f). By contrast, Fig. 5g–i do not show any relevant correlation between the radiation-induced bleaching of the 1610 cm^{-1} peak and the radiation-induced growth of the peaks in the 1627–1647 cm^{-1}, 2850–2925 cm^{-1}, and 3180–3390 cm^{-1} regions, whose increase cannot therefore be ascribed to a direct modification of the groups responsible for the 1610 cm^{-1} vibrational mode. Furthermore, the 1560 cm^{-1} peak, which is the only one showing a non-monotonic dependence between 0 and 100 Gy, does not manifest relevant correlation with other spectral features, but a moderate correlation with the 1627–1647 cm^{-1} peak pair (Fig. 5j-l). Further analysis of these vibrational modes – arising outside the PLA phonon spectrum and showing clear radiation-dependence and mutual relationships – can bring unprecedented information on the activated mechanisms. At this purpose, in the following lines, we briefly discuss their possible attribution to vibrational modes of specific molecular groups.

The pair at about 2850 and 2925 cm^{-1} (Fig. 3c) belongs to the region of C—H stretching modes [36]. The distinct spectral position with respect to the native C—H stretching modes of the CH_3 methyl groups in PLA, with peaks at 2880, 2945, and 2997 cm^{-1} [24], points to the attribution to C—H stretching modes in a modified PLA molecular unit. The strong correlation in Fig. 5b between the intensities of the two peaks suggests a common origin, and leads to the attribution to two vibrational modes of one group within the perturbed molecular unit. Indeed, their spectral positions are consistent with the formation of CH_2 groups, since peaks at about 2850 and 2925 cm^{-1} are observed from symmetric and asymmetric stretching modes of the methylene group, respectively, in several CH_2-containing materials (including polyethylene [37] and photodegraded PLA [38]).

The weak peaks at 3180 and 3390 cm^{-1} (Fig. 3c), in the region of the O—H vibrational modes, suggest the radiation-induced formation of hydroxyl groups. The hygroscopic nature of PLA can indeed cause the incorporation of a small amount of water molecules, which then react with the polymer during irradiation to form hydroxyl groups. The presence of native H_2O molecules in the set of PLA samples is indeed confirmed by the detection of a very broad, however weak, band in the 3100–3600 cm^{-1} region of the water stretching modes (Fig. 3a and c). It is to be remarked, however, that the 3180 and 3390 cm^{-1} peaks cannot be directly ascribed to incorporated water molecules, whose vibrational spectrum in the OH stretching region is not expected to give rise to narrow peaks (exceptions only regard water molecules in crystals with structural water or systems with water molecules in specific fixed sites of ordered lattices [39,40]). The narrow spectral features of the pair 3180 and 3390 cm^{-1} rather suggest the radiation-induced formation of in-chain OH groups within the PLA molecular unit. It is worth noting, indeed, that these groups are distinct from the OH end-groups of PLA chains, which are instead responsible for peaks at 3657 and 3510 cm^{-1} [33] that we indeed observed and that do not show any intensity change by irradiation (Fig. 3c).

The broad native peak at 1610 cm^{-1} (Fig. 3a and b) is ascribable to the δ(HOH) bending mode of water molecules, as observed in several systems and interfaces [41–43] and also in PLA interacting with water [44]. Alternative attributions of the 1610 cm^{-1} peak to stretching modes of amide groups or to C=C bonds in aromatic rings [36,45,46], on the other hand, are unlikely because no nitrogen contamination is detectable in the elemental analysis, and other characteristic vibrational modes of aromatic rings are absent but should show a narrower bandwidth than those observed in the present case.

The spectral region of C=C stretching of non-conjugated alkenes lies between 1620 and 1680 cm^{-1} [36,46], where the two narrow peaks at 1627 and 1647 cm^{-1} are observed in the present set of irradiated samples (Fig. 3b). Other works reported IR spectra of PLA, where one can

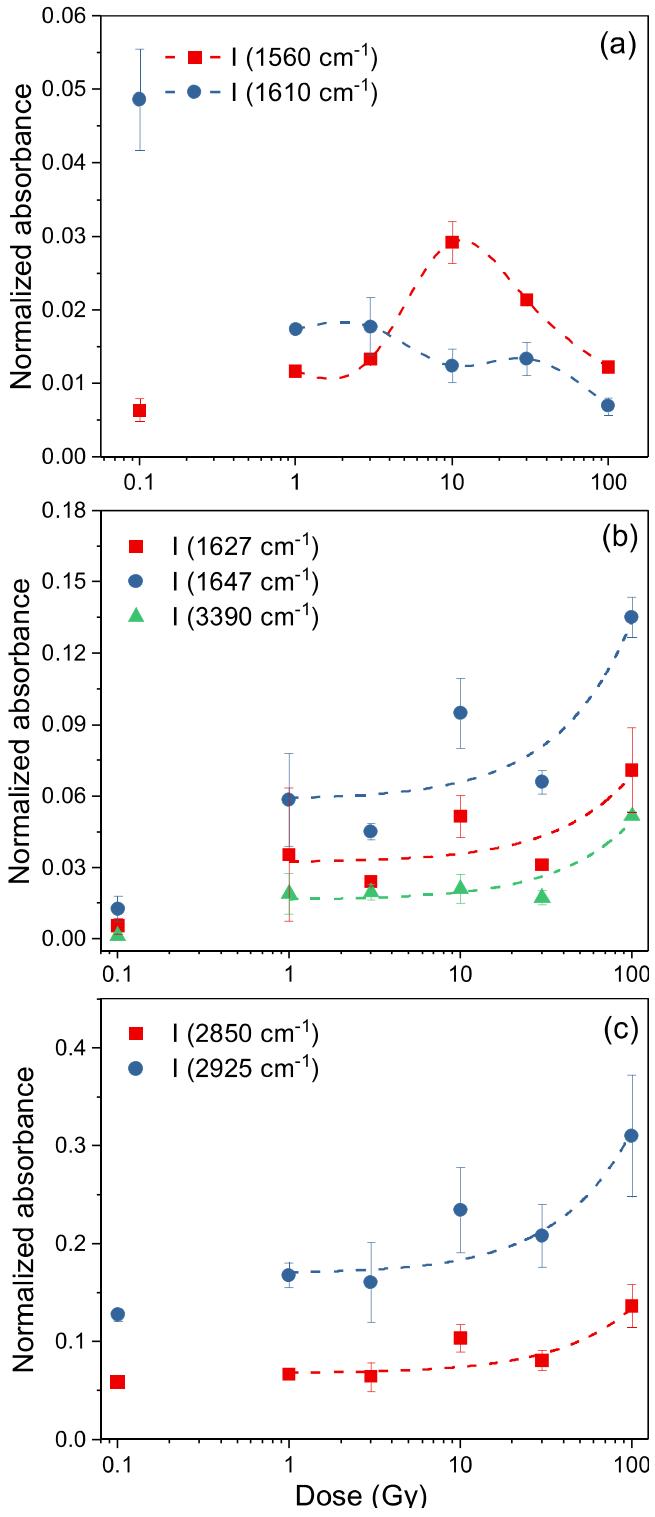

Fig. 4. Radiation dependence of anomalous vibrational peaks. ATR-FTIR intensity *vs.* x-ray dose in semi-logarithmic scale, compared with intensity in unirradiated samples, of (a) peaks at 1560 and 1610 cm^{-1}, (b) peaks at 1627, 1647, and 3390 cm^{-1}, (c) peaks at 2850 and 2925 cm^{-1}. All values are normalized to the intensity of the 1450 cm^{-1} peak of CH_3 bending mode in the same spectrum. Error bars are the standard deviation of the values in the data population. Dashed curves in (a) are a guide to the eye, whereas in (b) and (c) are the result of the linear fitting of the data.

find some evidence of minor spectral contributions at around 1640–1660 cm^{-1} [33,47–50], and a couple of these studies indeed associate the 1647 cm^{-1} peak with the formation of C=C bonds [49,50].

The attribution of the peak at 1560 cm^{-1} – excluding the involvement of amide groups, whose presence is not consistent with the data of elemental analysis – could point to the involvement of a perturbed configuration of carbonyl groups, as already suggested for PLA and other carbon-based systems after oxidation processes and the formation of hydrogen-bonding [36,50,51]. Since the investigated PLA samples show this spectral feature only at low irradiation doses, then disappearing at higher doses, the 1560 cm^{-1} peak probably emerges from an unstable intermediate perturbation of the molecular unit.

3.3. *Mechanisms of radiation-induced perturbation of the molecular unit*

The IR absorption data in the previous sections give evidence of a clear perturbation of the PLA molecular unit as an effect of x-ray irradiation in the investigated low-dose range. The molecular perturbation appears to involve the formation of chemical groups and bonds that are not originally part of the PLA molecular unit: (a) C=C bonds, (b) hydroxyl groups OH (distinct from chain-end groups), c) methylene -CH_2 groups, and d) hydrogen-bonding carbonyl groups C=O···H.

From these data, it appears that the initial events of radiation damage comprise different possible processes of molecular unit modification. A Norrish type-II mechanism has been proposed to take part in the PLA photodegradation processes [33,38,52], with the reaction products that include CH_2 and OH groups. However, this mechanism alone cannot explain the experimental results in some cases [38,52], and in the present set of data too. According to this mechanism, the CH_2 and OH groups would indeed result from the transfer of hydrogen from the methyl group to the carbonyl group, giving rise to alkene =CH_2 groups, whose characteristic modes at 3000–3100 cm^{-1} are not observed in our case. Interestingly, the first step of the Norrish type-II reaction, starting from the unperturbed PLA molecular unit, comprises the hydrogen-bonding of the carbonyl group with the methyl group (Fig. 6a, b). This mechanism appears to be consistent with a C=O stretching mode significantly lowered in frequency, down to the spectral region around 1560 cm^{-1}. The detection of the 1560 cm^{-1} peak after low-dose irradiation suggests the occurrence of Norrish type-II reaction in our samples as initial metastable step of radiation-induced changes in the molecular unit (Fig. 6b).

The next modification mechanisms must include the reaction of C=C bonds formation with the carbon atom of the carbonyl group and the transformation of the carbonyl group into an intrachain C—OH group (Fig. 6c). Indeed, the alternative formation of a C=C double bond with the carbon site of the methyl group must be excluded because it would imply the formation of =CH_2 groups, whose alkene C—H stretching modes in the range 3000–3100 cm^{-1} [36] are not present in the collected spectra. Instead, the hydroxylation of the carbonyl group is well supported by the emergence of the pair of peaks at 3180 and 3390 cm^{-1}. These peaks, which cannot be ascribed to hydroxyl sites at the chain end, can be interpreted as due to the stretching modes of OH groups in =COH—O structures involved in intramolecular hydrogen bonds within the molecular unit, as also observed in other systems [53, 54]. It is worth noting that this process appears like a keto-enol tautomerism [55] driven by radiation in the presence of water molecules. This process is indeed in agreement with the rise of C=C modes at 1627–1647 cm^{-1} and intrachain OH stretching at 3200–3400 cm^{-1}. Analogously to the typical mechanisms of keto-enol tautomerism, the formation of the hydroxyl group is likely to involve the reaction of water molecules, which are an alternative to, and possibly substituting for, the hydrogen-bonding between carbonyl and methyl groups in Fig. 6b. In such a case, the evolution is not a Norrish type-II reaction, which cannot account for the growth of -CH_2 stretching modes in the 2850–2930 cm^{-1} region. In fact, in parallel with the hydroxylation of the carbonyl group, the reaction with water molecules transforms the methyl -CH_3 group

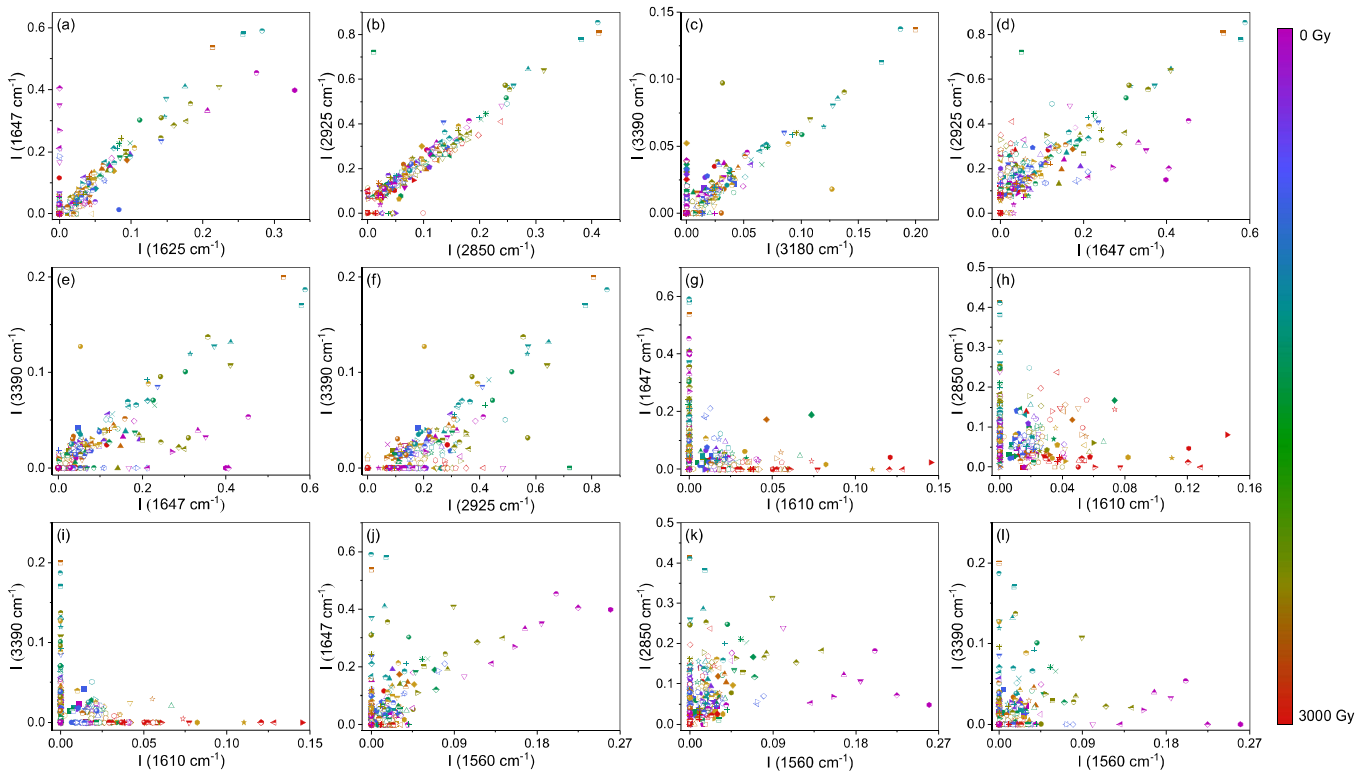

Fig. 5. Correlation plots. Intensity relations of the indicated anomalous infrared absorption peaks in the FTIR spectrum of irradiated and unirradiated PLA collected in 36 different measurement campaigns (labelled by different symbols) each concerning an average of 6 samples and repeated measurements on each sample. Intensity values are normalized to the intensity of the intrinsic CH_3 bending mode of PLA at 1450 cm^{-1} as an internal reference in each collected spectrum.

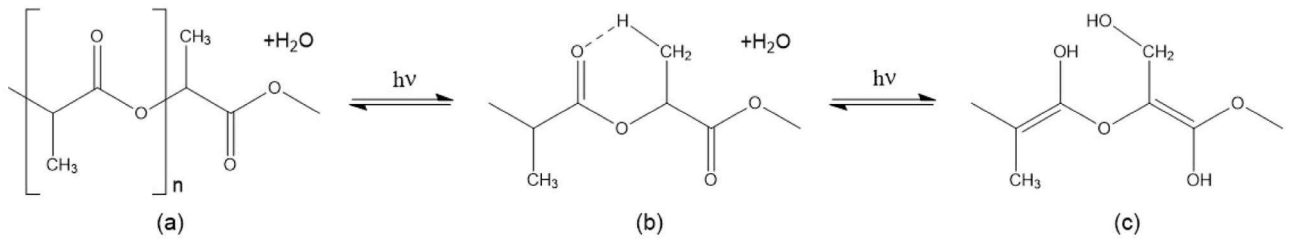

Fig. 6. Mechanisms of modification. (a) PLA molecular unit and adsorbed water. (b) Methyl-carbonyl hydrogen bonding in a Norrish II-like reaction. (c) Final structure from the reaction with a water molecule, with the formation of alkene CH_2 and intrachain OH, together with C=C bonds.

into a -CH_2—OH group, consistent with the emergence of the pair of peaks at 2850–2925 cm^{-1} (Fig. 6c). Importantly, this type of mechanism does not involve chain breakage, in agreement with the lack of detectable increase of signal from end-chain OH groups. GPC measurements of molecular weight before and after irradiation confirm the lack of M_w modification ascribable to chain breaking. Further independent confirmation of the lack of chain breaking comes from ^{1}H NMR measurements on samples obtained from unirradiated and irradiated material. After verifying by FTIR the full removal of interfering sidechain OH groups by PLLA dissolution in $CHCl_3$ (Fig. S6a), no relevant difference of OH resonance intensity at about 3.5 ppm does indeed result from irradiation (Fig. S6b), therefore ruling out an increase of end-chain OH by chain breaking.

3.4. Evolution at high doses and thermal stability of modified groups

The modified molecular unit in Fig. 6b – with an intrachain hydrogen bond between methyl and carbonyl groups – is unstable, as evidenced by the decrease in the IR mode at 1560 cm^{-1} at doses above 10 Gy (Fig. 4a). This fact suggests that the intermediate state in Fig. 6b can proceed either back to the initial state of the polymer or to different conformational states, including the occurrence of possible reactions with water molecules (Fig. 6c) and subsequent interactions with other groups. At higher irradiation doses, even the other radiation-induced IR modes show to be metastable. At doses higher than 100 Gy up to 3 kGy, all radiation-induced IR modes show a decrease to very low asymptotic values (Fig. S7), suggesting the occurrence of processes of energy release from the radiation to the material resulting in the annealing of the groups created in the first steps of the modification of the PLA molecular unit.

The data of isochronous and isothermal annealing of the radiation-induced modes in the IR spectra confirm the thermal instability of the radiation-induced groups and support the role of the mechanisms of thermal energy release during x-ray exposure. In fact, Fig. 7 shows that the 1627–1647 cm^{-1} peaks are bleached after thermal heating to above 60 °C, just in the range of the PLA glass transition temperature, down to negligible values after annealing at 80 °C, with similar results for the other peaks. This fact suggests that the bleaching of the radiation-induced vibrational modes is caused by interchain interactions promoted by heating above the glass transition temperature of the system.

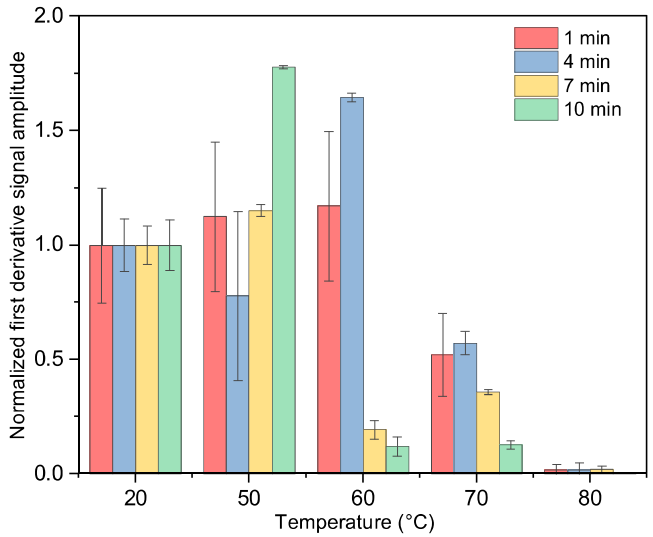

Fig. 7. Thermal stability of anomalous peaks. First derivative ATR-FTIR intensity *vs.* annealing temperature for different annealing times of the 1647 cm^{-1} peak normalized to the starting intensity (unitary value at 20 °C). Error bars are estimated from the signal-to-noise ratio of the IR spectra.

Importantly, if the reduction in intensity at high doses is the result of interchain reactions, a conformational change should occur. Evidence of such an effect indeed comes from DSC measurements we have collected on irradiated samples at different irradiation doses (Fig. S8 and Table S1) looking at possible changes of the glass transition temperature.

Fig. 8 reports the data of the glass transition temperature *vs.* dose, displaying a lowering of T_g at irradiation doses above 100 Gy. These data indeed support the occurrence of a conformational readjustment in the material irradiated at doses above 100 Gy, just in that dose range that shows the disappearance of the anomalous vibrational modes that arise during the initial events of modification of the PLA molecular unit. A rearrangement of the conformational structure toward a less crystalline state is therefore demonstrated, likely driven by interchain interactions mediated by reaction between radiation-induced molecular groups and by local energy release by x-ray beam.

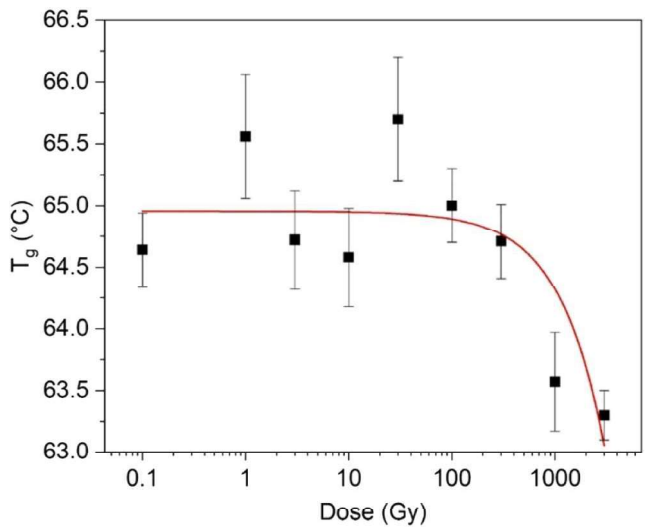

Fig. 8. Dose dependence of the glass transition temperature. Glass transition temperature *vs.* x-ray dose in semi-logarithmic scale, as obtained from DSC curves on irradiated PLA samples. The curve is a guide to the eye. Error bars are obtained from the propagation of temperature uncertainty in the standard DSC curve analysis process to determine the T_g.

3.5. Role of the initial conformation

The comparison between samples with different initial conformation shows strong differences in the effects of irradiation, as exemplified in Fig. 9 in the case of the 1647 cm-1 mode after 100 Gy irradiation. Relevant intensities are reported for AE and CC type materials, which possess more crystalline features, whereas the amorphous variants (MQ, RM, and RE) show negligible intensities. Importantly, all other structural and compositional features are comparable among the different variants since they were obtained from the same batch of material through controlled thermal treatments.

In other words, the initial events of modification of the PLA molecular units result to be strongly hindered by an amorphous initial conformation. As regards the possible causes of this hindering, it is worth noting that amorphous and crystalline PLA show almost equal water molecule diffusion coefficient and solubility [56], which cannot therefore be largely responsible for the observed effect. On the other hand, since amorphous and crystalline PLA variants mainly differ for the packing of the helical chains, the source of such an effect should be looked for in how the different interactions between chains hinder or promote the reaction in Fig. 6. Along this line, the results in Fig. 9 suggest that the initial reaction of methyl-carbonyl hydrogen bonding (Fig. 6b) are relevantly promoted by a specific surrounding of these groups, namely the surrounding occurring in the α crystalline phase. Further computational studies will be useful to check this point. As a result of the observed role of crystallinity, it is to be noticed that – despite the observed effects basically involve intra-molecular mechanisms which are probably scarcely dependent on the molecular weight – an indirect effect of molecular weight could however be expected as far as it can influence the crystallization propensity.

4. Conclusions

The present investigation gives the first experimental overview on the PLA modification by very low doses of ionizing irradiation, leading to identify the initial events of perturbation of the molecular unit. The spectroscopic results provide a new insight into the radiation-activated groups which prepare the material for the conformational and morphological evolution at high irradiation doses.

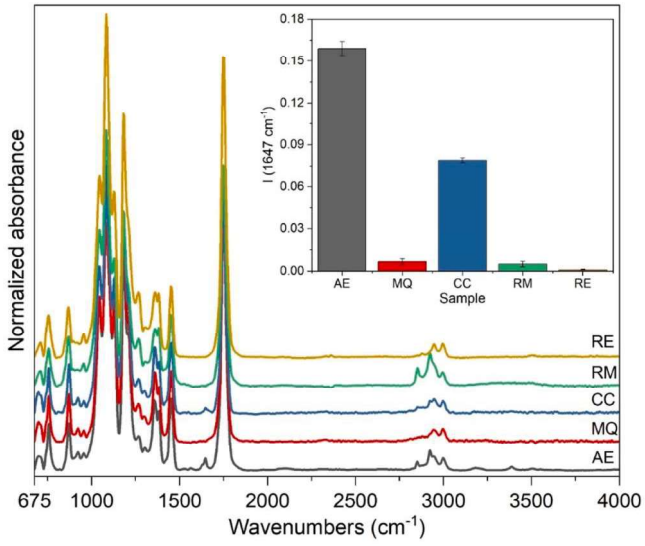

Fig. 9. Conformation dependence. Representative ATR-FTIR spectra after 100Gy x-ray exposure of different types of PLA samples (labels as in Fig. 2). Intensities are normalized to the intrinsic CH_3 bending mode at 1450 cm^{-1}. Inset: Intensity values of the x-ray induced 1647 cm^{-1} mode in the different representative samples.

Evidence is obtained on the formation of C=C groups in the backbone, accompanied by the transformation of methyl groups to alkene CH_2 groups and the hydroxylation of carbonyl groups. These mechanisms do not cause relevant processes of chain scission, which instead occur in regimes with much higher irradiation doses, as reported in the literature. However, during prolonged irradiation, the groups activated by radiation disappear and drive the polymer chains towards conformational rearrangements, as evidenced by a decrease in the glass transition temperature. Interestingly, the activation of the observed mechanisms at low doses is hindered by the decrease in the crystalline features of the material, providing an indication of the role of the conformation in PLA radiation hardness and in triggering damage to the molecular unit. These results could suggest best practices to optimize PLA-based materials for specific applications – depending on desired radiation hardness and biodegradability – based on suitable treatments of thermal crystallization or amorphization or irradiation. Importantly, along this way, new processes of PLA production could be designed with improved features for applications which involve radiation exposure.

CRediT authorship contribution statement

Giulia Tamburini: Conceptualization, Formal analysis, Investigation, Visualization, Writing – review & editing. **Stefano Bertagnoli:** Resources. **Giulia Tarricone:** Investigation. **Sergio Piva:** Investigation. **Adele Sassella:** Conceptualization, Writing – review & editing. **Roberto Lorenzi:** Methodology, Writing – review & editing, Supervision. **Alberto Paleari:** Conceptualization, Methodology, Writing – original draft, Project administration.

Declaration of Competing Interest

The authors declare that they have no known competing financial interests or personal relationships that could have appeared to influence the work reported in this paper.

Data availability

Data will be made available upon reasonable request.

Acknowledgments

G.T. gratefully acknowledges the financial support from the Ministry of the Research and University and from Galatea Bio Tech srl (Project FSE REACT-EU, IV.5 Action, DM 1061/2021). The authors thank F. Maspero for kindly performing elemental analysis of the material.

Supplementary materials

Supplementary material associated with this article can be found, in the online version, at doi:10.1016/j.polymdegradstab.2023.110485.

References

[1] A. Ashfaq, M.C. Clochard, X. Coqueret, C. Dispenza, M.S. Driscoll, P. Ulański, M. Al-Sheikhly, Polymerization Reactions and Modifications of Polymers by Ionizing Radiation, Polymers 12 (2020) 2877, https://doi.org/10.3390/polym12122877 (Basel).

[2] S. Ho, W.Y. Lau, T.W.T. Leung, M. Chan, P.J. Johnson, A.K.C. Li, Clinical evaluation of the partition model for estimating radiation doses from yttrium-90 microspheres in the treatment of hepatic cancer, Eur. J. Nucl. Med. 24 (1997) 293–298, https://doi.org/10.1007/BF01728766.

[3] J.S. Welsh, Radiographically identified necrosis after 90y microsphere brachytherapy: a new standard for oncologic response assessment? AJR 188 (2007) 765–767, https://doi.org/10.2214/AJR.07.5320.

[4] G.N. Atroshchenko, V.I. Savinkov, A. Paleari, P.D. Sarkisov, V.N. Sigaev, Glassy microspheres with elevated yttrium oxide content for nuclear medicine, Glass Ceram. 69 (2012) 39–43, https://doi.org/10.1007/s10717-012-9410-8.

[5] V.N. Sigaev, G.N. Atroschenko, V.I. Savinkov, P.D. Sarkisov, G. Babajew, K. Lingel, R. Lorenzi, A. Paleari, Structural rearrangement at the yttrium-depleted surface of HCl-processed yttrium alumino-silicate glass for 90Y-microsphere brachytherapy, Mater. Chem. Phys. 133 (2012) 24–28, https://doi.org/10.1016/j.matchemphys.2011.12.079.

[6] K. Saralidze, L.H. Koole, M.L.W. Knetsch, Polymeric microspheres for medical applications, Materials 3 (6) (2010) 3537–3564, https://doi.org/10.3390/ma3063537 (Basel).

[7] M. Rahimi, G. Charmi, K. Matyjaszewski, X. Banquy, J. Pietrasik, Recent developments in natural and synthetic polymeric drug delivery systems used for the treatment of osteoarthritis, Acta Biomater. 123 (2021) 31–50, https://doi.org/10.1016/j.actbio.2021.01.003.

[8] P. Jana, M. Shyam, S. Singh, V. Jayaprakash, A. Dev, Biodegradable polymers in drug delivery and oral vaccination, Eur. Polym. J. 142 (2021), 110155, https://doi.org/10.1016/j.eurpolymj.2020.110155.

[9] T. Casalini, F. Rossi, A. Castrovinci, G. Perale, A perspective on polylactic acid-based polymers use for nanoparticles synthesis and applications, Front. Bioeng. Biotechnol. 7 (2019) 259, https://doi.org/10.3389/fbioe.2019.00259.

[10] S. Pérez Davila, L. González Rodríguez, S. Chiussi, J. Serra, P González, How to sterilize polylactic acid based medical devices? Polymers 13 (2021) 2115, https://doi.org/10.3390/polym13132115 (Basel).

[11] R.J. Mumper, U.Y. Ryo, M. Jay, Neutron-activated holmium- 166-poly (L-lactic acid) microspheres: a potential agent for the internal radiation therapy of hepatic tumors, J. NucI. Med. 32 (1991) 2139–2143.

[12] J.F.W. Nijsen, B.A. Zonnenberg, J.R.W. Woittiez, D.W. Rook, I.A. Swildens-van Woudenberg, P.P. van Rijk, A.D. van het Schip, Holmium-166 poly lactic acid microspheres applicable for intra-arterial radionuclide therapy of hepatic malignancies: effects of preparation and neutron activation techniques, Eur. J. Nucl. Med. 26 (7) (1999) 699–704, https://doi.org/10.1007/s002590050440.

[13] J.F.W. Nijsen, Radioactive Holmium Poly(L-Lactic Acid) Microspheres for Treatment of Liver Malignancies, Utrecht University, The Netherlands, 2001.

[14] J.F.W. Nijsen, A.D. van het Schip, M.J. van Steenbergen, S.W. Zielhuis, L.M. J. Kroon-Batenburg, M. van de Weert, P.P. van Rijk, W.E. Hennink, Influence of Neutron Irradiation on Holmium Acetylacetonate Loaded Poly(L -Lactic Acid) Microspheres, Biomaterials 23 (8) (2002) 1831–1839, https://doi.org/10.1016/S0142-9612(01)00309-X.

[15] S.W. Zielhuis, J.F.W. Nijsen, R. de Roos, G.C. Krijger, P.P. van Rijk, W.E. Hennink, A.D. van het Schip, Production of GMP-grade radioactive holmium loaded poly(L-lactic acid) microspheres for clinical application, Int. J. Pharm. 311 (1–2) (2006) 69–74, https://doi.org/10.1016/j.ijpharm.2005.12.034.

[16] M. Jamre, M. Shamsaei, M. Ghannadi-Maragheh, S. Sadjadi, Novel 175Yb-poly (L-lactic acid) microspheres for transarterial radioembolization of unrespectable hepatocellular carcinoma, Iran. J. Pharm. Res. 18 (2) (2019) 569–578, https://doi.org/10.22037/ijpr.2019.1100668.

[17] Y. Yıldırım, A. Oral, The influence of γ-ray irradiation on the thermal stability and molecular weight of Poly(L-Lactic acid) and its nanocomposites, Radiat. Phys. Chem. 96 (2014) 69–74, https://doi.org/10.1016/j.radphyschem.2013.08.016.

[18] M.L. Cairns, G.R. Dickson, J.F. Orr, D. Farrar, C. Hardacre, J. Sa, P. Lemoine, M. Z. Mughal, F.J. Buchanan, The potential of electron beam radiation for simultaneous surface modification and bioresorption control of PLLA, J. Biomed. Mater. Res. Part A 100A (2012) 2223–2229, https://doi.org/10.1002/jbm.a.34156.

[19] T.A.M. Valente, D.M. Silva, P.S. Gomes, M.H. Fernandes, J.D. Santos, V. Sencadas, Effect of sterilization methods on electrospun poly(lactic acid) (PLA) fiber alignment for biomedical applications, ACS Appl. Mater. Interfaces 8 (2016) 3241–3249, 10.1021/acsami.5b10869.

[20] T.J. Madera-Santana, R. Meléndrez, G. González-García, P. Quintana-Owen, S. D. Pillai, Effect of gamma irradiation on physicochemical properties of commercial poly(lactic acid) clamshell for food packaging, Radiat. Phys. Chem. 123 (2016) 6–13, https://doi.org/10.1016/j.radphyschem.2016.02.001.

[21] E.C. Grosvenor, J.C. Hughes, C.W. Stanfield, R.L. Blanchard, A.C. Fox, O.L. Mihok, K. Lee, J.R. Brodsky, A. Hoy, A. Uniyal, S.M. Whitaker, C. Acha, K. Gibson, L. Ding, C.A. Lewis, L. González López, C.M. Wentz, L.R. Sita, M. Al-Sheikhly, On the mechanism of electron beam radiation-induced modification of poly(lactic acid) for applications in biodegradable food packaging, Appl. Sci. 12 (2022) 1819, https://doi.org/10.3390/app12041819.

[22] M. Rzepna, J. Sadło, G. Przybytniak, A. Iuliano, Impact of electron beam treatment on copolymers of polylactide and poly(trimethylene carbonate) in an air atmosphere, J. Appl. Polym. Sci. 138 (2021) e50184, https://doi.org/10.1002/app.50184.

[23] A. Adamus-Wlodarczyk, R.A. Wach, P. Ulanski, J.M. Rosiak, M. Socka, Z. Tsinas, M. Al-Sheikhly, On the mechanisms of the effects of ionizing radiation on Diblock and random copolymers of poly(lactic acid) and poly(trimethylene carbonate), Polymers 10 (2018) 672, https://doi.org/10.3390/polym10060672 (Basel).

[24] G. Kister, G. Cassanas, M. Vert, Effects of morphology, conformation and configuration on the IR and Raman spectra of various poly(lactic acid)s, Polymer 39 (2) (1998) 267–273, https://doi.org/10.1016/S0032-3861(97)00229-2 (Guildf).

[25] S. Kang, S.L. Hsu, H.D. Stidham, P.B. Smith, M.A. Leugers, X. Yang, A spectroscopic analysis of poly(lactic acid) structure, Macromol 34 (2001) 4542–4548, https://doi.org/10.1021/ma0016026.

[26] L. Zaidi, S. Bruzaud, M. Kaci, A. Bourmaud, N. Gautier, Y. Grohens, The effects of gamma irradiation on the morphology and properties of polylactide/cloisite 30B nanocomposites, Polym. Degrad. Stab. 98 (2013) 348–355, https://doi.org/10.1016/j.polymdegradstab.2012.09.014.

[27] I. Zembouai, M. Kaci, S. Bruzaud, I. Pillin, J.L. Audic, S. Shayanfar, S.D. Pillai, Electron beam radiation effects on properties and ecotoxicity of PHBV/PLA blends in presence of organo-modified montmorillonite, Polym. Degrad. Stab. 132 (2016) 117–126, https://doi.org/10.1016/j.polymdegradstab.2016.03.019.
[28] T. Aouat, M. Kaci, J.M. Lopez-Cuesta, E.,. Devaux, M. Mahlous, The effect of gamma-irradiation on morphology and properties of melt-spun poly (lactic acid)/cellulose fibers, Polym. Degrad. Stab. 160 (2019) 14–23, https://doi.org/10.1016/j.polymdegradstab.2018.11.014.
[29] M. Vidotto, B. Mihaljević, G. Žauhar, E. Vidović, N. Maltar-Strmečki, D. Klepac, S. Valić, Effects of γ-radiation on structure and properties of poly(lactic acid) filaments, Radiat. Phys. Chem. 184 (2021), 109456, https://doi.org/10.1016/j.radphyschem.2021.109456.
[30] S.C.J. Loo, C.P. Ooi, Y.C.F. Boey, Radiation effects on poly(lactide-co-glycolide) (PLGA) and poly(L-lactide) (PLLA), Polym. Degrad. Stab. 83 (2004) 259–265, https://doi.org/10.1016/S0141-3910(03)00271-4.
[31] M.L. Cairns, G.R. Dickson, J.F. Orr, D. Farrar, K. Hawkins, F.J. Buchanan, Electron-beam treatment of poly(lactic acid) to control degradation profiles, Polym. Degrad. Stab. 96 (2011) 76–83, https://doi.org/10.1016/j.polymdegradstab.2010.10.016.
[32] A. Babanalbandi, D.J.T. Hill, J.H. O'Donnell, P.J. Pomery, An electron spin resonance analysis on y-irradiated poly(glycolic acid) and its copolymers with lactic acid, Polym. Degrad. Stab. 52 (1996) 59–66, 10.1016/0141-3910(95)00230-8.
[33] E. Olewnik-Kruszkowska, I. Kotera, J. Skopińska-Wiśniewska, J. Richert, Degradation of polylactide composites under UV irradiation at 254nm, J. Photochem. Photobiol. A Chem. 311 (2015) 144–153, https://doi.org/10.1016/j.jphotochem.2015.06.029.
[34] J. Kowalonek, I. Vuković-Kwiatkowska, D. Moszyński, H. Kaczmarek, Surface properties of poly(lactic acid)/polyacrylate semi-interpenetrating networks – Effect of UVC radiation, Polym. Degrad. Stab. 131 (2016) 71–81, https://doi.org/10.1016/j.polymdegradstab.2016.07.008.
[35] D. Brizzolara, H.J. Cantow, K. Diederichs, E. Keller, A.J. Domb, Mechanism of the stereocomplex formation between enantiomeric poly(lactide)s, Macromolecules 29 (1996) 191–197, https://doi.org/10.1021/ma951144e.
[36] G. Socrates, Infrared and Raman Characteristic Group Frequencies, Tables and Charts, John Wiley & Sons, Ltd, Baffins Lane, Chichester UK, 2001.
[37] M. Bredács, C. Barretta, L.F. Castillon, A. Frank, G. Oreski, G. Pinter, S. Gergely, Prediction of polyethylene density from FTIR and Raman spectroscopy using multivariate data analysis, Polym. Test. 104 (2021), 107406, 1016/j.polymertesting.2021.107406.
[38] S. Bocchini, K. Fukushima, A. Di Blasio, A. Fina, A. Frache, F. Geobaldo, Polylactic Acid and Polylactic Acid-Based Nanocomposite Photooxidation, Biomacromol 11 (2010) 2919–2926, https://doi.org/10.1021/bm1006773.
[39] L. Nasdala, A. Beran, E. Libowitzky, D. Wolf, The incorporation of hydroxyl groups and molecular water in natural zircon ($ZrSiO_4$), Am. J. Sci. 301 (2001) 831–857, https://doi.org/10.2475/ajs.301.10.831.
[40] J.W. Cao, J.Y. Chen, X.L. Qin, X.L. Zhu, L. Jiang, Y. Gu, X.H. Yu, P. Zhang, DFT investigations of the vibrational spectra and translational modes of ice II, Molecules 24 (2019) 3135, https://doi.org/10.3390/molecules24173135.
[41] Z. Wang, A. Pakoulev, Y. Pang, D.D. Dlott, Vibrational substructure in the OH stretching transition of water and HOD, J. Phys. Chem. A 108 (2004) 9054–9063, https://doi.org/10.1021/jp048545t.
[42] T. Seki, K.Y. Chiang, C.C. Yu, X. Yu, M. Okuno, J. Hunger, Y. Nagata, M. Bonn, The bending mode of water: a powerful probe for hydrogen bond structure of aqueous systems, J. Phys. Chem. Lett. 11 (2020) 8459–8469, https://doi.org/10.1021/acs.jpclett.0c01259.
[43] H. Hanawa, K. Kunimatsu, M. Watanabe, H. Uchida, In situ ATR-FTIR analysis of the structure of nafion−Pt/C and nafion−Pt_3Co/C interfaces in fuel cell, J. Phys. Chem. C 116 (2012) 21401–21406, https://doi.org/10.1021/jp306955q.
[44] O. Vyavahare, D. Ng, S.L. Hsu, Analysis of structural rearrangements of Poly(lactic acid) in the presence of water, J. Phys. Chem. B 118 (2014) 4185–4193, https://doi.org/10.1021/jp500219.
[45] R. Brudler, H.J.M. de Groot, W.B.S. van Liemt, W.F. Steggerda, R. Esmeijer, P. Gast, A.J. Hoff, J. Lugtenburg, K. Gerwert, Asymmetric binding of the 1- and 4-C=O groups of Q_A in Rhodobacter sphaeroides R26 reaction centres monitored by Fourier transform infra-red spectroscopy using site-specific isotopically labelled ubiquinone-10, EMBO J. 13 (23) (1994) 5523–5530, https://doi.org/10.1002/j.1460-2075, 1994.tb06889.x.
[46] A.M. Herrera-González, M. Caldera-Villalobos, A.A. Pérez-Mondragón, C. E. Cuevas-Suárez, J.A. González-López, Analysis of double bond conversion of photopolymerizable monomers by FTIR-ATR spectroscopy, J. Chem. Educ. 96 (2019) 1786–1789, https://doi.org/10.1021/acs.jchemed.8b00659.
[47] A. Alsabbagh, R.A. Saleem, R. Almasri, S. Aljarrah, S. Awad, Effects of gamma irradiation on 3D-printed polylactic acid (PLA) and high-density polyethylene (HDPE), Polym. Bull. 78 (2021) 4931–4945, https://doi.org/10.1007/s00289-020-03349-3.
[48] J.R. Rocca-Smith, T. Karbowiak, E. Marcuzzo, A. Sensidoni, F. Piasente, D. Champion, O. Heinz, P. Vitry, E. Bourillot, E. Lesniewska, F. Debeaufort, Impact of corona treatment on PLA film properties, Polym. Degrad. Stab. 132 (2016) 109–116, https://doi.org/10.1016/j.polymdegradstab.2016.03.020.
[49] T. Saiga, S. Sato, K. Nagai, Water vapor solubility of poly(lactic acid) films modified the surface by vacuum ultraviolet irradiation, J. Appl. Polym. Sci. 132 (2015) 42200, https://doi.org/10.1002/app.42200.
[50] C. West, R. McTaggart, T. Letcher, D. Raynie, R. Roy, Effects of gamma irradiation upon the mechanical and chemical properties of 3D-printed samples of polylactic acid, J. Manuf. Sci. Eng. 141 (2019), https://doi.org/10.1115/1.4042581, 041002-1.
[51] F. Navarro-Pardo, G. Martínez-Barrera, A.L. Martínez-Hernández, V.M. Castaño, J. L. Rivera-Armenta, F. Medellín-Rodríguez, C. Velasco-Santos, Effects on the thermo-mechanical and crystallinity properties of nylon 6,6 electrospun fibres reinforced with one dimensional (1d) and two dimensional (2D) carbon, Materials 6 (2013) 3494–3513, https://doi.org/10.3390/ma6083494 (Basel).
[52] Photodegradation behaviors of aliphatic polyesters, J. Photopolym. Scl. Tech 10 (1997) 265–270, https://doi.org/10.2494/photopolymer.10.265.
[53] A. Fujii, E. Fujimaki, T. Ebata, N.A. Mikami, New type of intramolecular hydrogen bonding: hydroxyl-methyl interactions in the o-cresol cation, J. Am. Chem. Soc. 120 (50) (1998) 13256–13257, https://doi.org/10.1021/ja982922w.
[54] A. Ramírez-Hernández, C. Aguilar-Flores, Aparicio-Saguilán, A. Fingerprint analysis of FTIR spectra of polymers containing vinyl acetate, Dyna 86 (209) (2019) 198–205, https://doi.org/10.15446/dyna.v86n209.77513 (Medellin).
[55] S. Ghorai, A. Laskin, A.V. Tivanski, Spectroscopic evidence of keto-enol tautomerism in deliquesced malonic acid particles, J. Phys. Chem. A 115 (2011) 4373–4380, https://doi.org/10.1021/jp112360x.
[56] J.S. Yoon, H.W. Jung, M.N. Kim, E.S. Park, Diffusion coefficient and equilibrium solubility of water molecules in biodegradable polymers, J. Appl. Polymer Sci. 77 (2000) 1716–1722, https://doi.org/10.1002/1097-4628(20000822)77:8<1716::AID-APP8>3.0.CO;2-F. AID-APP8≥3.0.CO,2-F.